Bioorganic & Medicinal Chemistry Letters 23 (2013) 4875–4885

Contents lists available at SciVerse ScienceDirect

Bioorganic & Medicinal Chemistry Letters

journal homepage: www.elsevier.com/locate/bmcl

Identification of 2,3-dihydro-1*H*-pyrrolo[3,4-*c*]pyridine-derived ureas as potent inhibitors of human nicotinamide phosphoribosyltransferase (NAMPT)

Peter S. Dragovich [a,*], Kenneth W. Bair [b], Timm Baumeister [b], Yen-Ching Ho [b], Bianca M. Liederer [a], Xiongcai Liu [c], Yongbo Liu [c], Thomas O'Brien [a], Jason Oeh [a], Deepak Sampath [a], Nicholas Skelton [a], Leslie Wang [a], Weiru Wang [a], Hongxing Wu [c], Yang Xiao [a], Po-wai Yuen [c], Mark Zak [a], Lei Zhang [c], Xiaozhang Zheng [b]

[a] *Genentech Inc., 1 DNA Way, South San Francisco, California 94080, USA*
[b] *Forma Therapeutics Inc., 500 Arsenal Street, Watertown, Massachusetts 02472, USA*
[c] *Pharmaron Beijing Co. Ltd., 6 Taihe Road, BDA, Beijing 100176, PR China*

ARTICLE INFO

Article history:
Received 4 May 2013
Revised 14 June 2013
Accepted 27 June 2013
Available online 6 July 2013

Keywords:
Nicotinamide phosphoribosyltransferase
NAMPT
Aqueous solubility
X-ray crystal structure
Tumor metabolism

ABSTRACT

Potent nicotinamide phosphoribosyltransferase (NAMPT) inhibitors containing 2,3-dihydro-1*H*-pyrrolo[3,4-c]pyridine-derived ureas were identified using structure-based design techniques. The new compounds displayed improved aqueous solubilities, determined using a high-throughput solubility assessment, relative to previously disclosed urea and amide-containing NAMPT inhibitors. An optimized 2,3-dihydro-1*H*-pyrrolo[3,4-c]pyridine-derived compound exhibited potent anti-NAMPT activity (**18**; BC NAMPT IC_{50} = 11 nM; PC-3 antiproliferative IC_{50} = 36 nM), satisfactory mouse PK properties, and was efficacious in a PC-3 mouse xenograft model. The crystal structure of another optimized compound (**29**; NAMPT IC_{50} = 10 nM; A2780 antiproliferative IC_{50} = 7 nM) in complex with the NAMPT protein was also determined.

Nicotinamide phosphoribosyltransferase (NAMPT; also known in the literature as pre-B cell colony-enhancing factor/PBEF and visfatin) catalyzes the condensation of nicotinamide (NAM) and phosphoribosyl pyrophosphate (PRPP) to produce nicotinamide mononucleotide (NMN; Fig. 1).[1] This transformation is dependent on the phosphorylation of a histidine residue in the NAMPT active site by ATP, and is the rate-limiting event in the two-step conversion of NAM to the important enzyme co-factor nicotinamide adenine dinucleotide (NAD; Fig. 1).[2] The NAM–NAD conversion represents the only known mechanism for mammalian cells to efficiently produce NAD from NAM that is liberated by NAD-consuming enzymes such as PARPs and Sirtuins.[3] Accordingly, NAMPT plays a key role in maintaining appropriate intracellular NAD levels, and blocking NAMPT activity may thus impair the growth and/or function of cells which are highly reliant on NAD-dependent processes for survival. Given the elevated metabolisms and high proliferation rates associated with many tumors and/or cancer cell lines, NAMPT inhibition is currently viewed as a novel strategy for the development of new anticancer agents.[4,5]

We previously described the identification of urea-containing NAMPT inhibitors exemplified by general structure **1** (Fig. 2) and compound **5** (Table 1).[6–8,32] We also disclosed the preparation of NAMPT inhibitors bearing amides derived from various bicyclic heteroaromatic moieties (e.g., structures **2** and **3**, Figure 2 and compounds **6** and **7**, Table 1).[9] Many examples of both the urea-containing inhibitors and the heteroaromatic compounds exhibited desirable biological properties including potent NAMPT inhibition activity, acceptable oral bioavailability, and efficacy in mice bearing human tumor xenografts. However, compounds from both of these inhibitor classes often displayed poor aqueous solubilities which complicated their further development. We therefore hypothesized that the introduction of a urea derived from a cyclic, aliphatic amine into the inhibitor design (structure **4**, Fig. 2) might favorably alter intra/inter hydrogen bonding characteristics relative to ureas such as **1** and thereby improve aqueous solubility properties. This design modification also involved the saturation of an aromatic ring present in structures **2** and **3**, and such alterations were also anticipated to beneficially impact

* Corresponding author.
E-mail address: dragovich.peter@gene.com (P.S. Dragovich).

0960-894X/$ - see front matter © 2013 Elsevier Ltd. All rights reserved.
http://dx.doi.org/10.1016/j.bmcl.2013.06.090

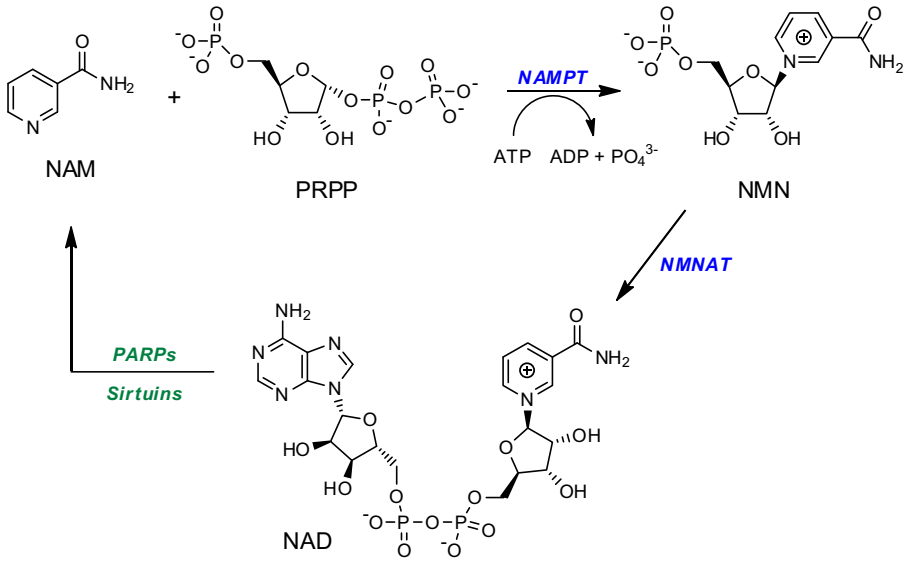

Figure 1. NAD recycling and NAMPT biochemical mechanism.

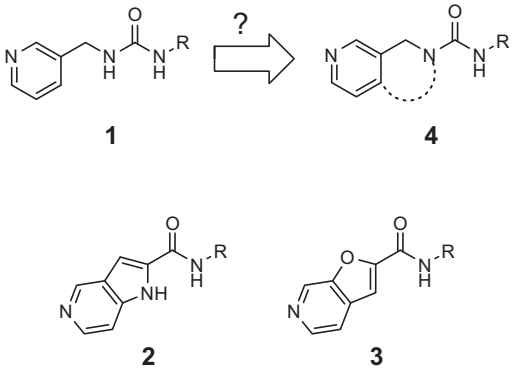

Figure 2. Design of ureas derived from cyclic, aliphatic amines as NAMPT inhibitors.

solubility parameters.[10] In this work, we describe the identification of NAMPT inhibitors bearing such aliphatic urea moieties as well as the subsequent transformation of the initial lead molecules into more optimized compounds.[11]

As shown in Table 1, an inhibitor containing a urea moiety derived from 2,3-dihydro-1*H*-pyrrolo[3,4-c]pyridine exhibited potent anti-NAMPT properties in both biochemical and cell culture assessments (compound **8**).[12] The compound's antiproliferation effects were ameliorated by the addition of 0.33 mM of NMN (the product of NAMPT catalysis; c.f., Fig. 1) to the cell assay, strongly implicating NAMPT inhibition as the causative mechanism. Importantly, the molecule also displayed improved aqueous solubility relative to our previously characterized NAMPT inhibitors bearing unsubstituted ureas or heteroaromatic amides (compare to compounds **5**, **6**, and **7**; Table 1).[13] Introduction of an amino substituent adjacent to the pyridine nitrogen atom present in **8** significantly worsened NAMPT inhibition and solubility properties (compound **9**). Relocation or removal of the pyridine nitrogen atom contained within **8** afforded molecules (**10** and **11**) which retained potent NAMPT biochemical inhibition properties but which were devoid of anti-NAMPT cell activity. This phenomenon likely arises from the inability of these compounds to form PRPP-derived phosphoribosylated adducts in the NAMPT active site.[14] Incorporation of larger aliphatic rings into the urea inhibitor design (compounds **12** and **13**, Table 1) was not tolerated, likely due to tight steric constraints in the NAMPT active site. Similarly, replacing the urea moiety present in **8** with the corresponding sulfonyl urea functional group led to complete loss of biological activity (compound **14**, Table 1). The above SAR studies identified the 2,3-dihydro-1*H*-pyrrolo[3,4-c]pyridine-derived urea as optimal for obtaining potent biochemical and cell-based NAMPT inhibition properties, and this functionality was therefore incorporated into all molecules described in the remainder of this work.

We next explored variation of the biaryl sulfone moiety present in compound **8**. As shown in Table 2, numerous substituted aromatic and heteroaromatic groups were tolerated at the inhibitor terminus (compounds **15**–**21**). These results paralleled those from our previous SAR studies of related NAMPT inhibitors and were consistent with this portion of the molecules residing in a solvent-exposed region in the NAMPT binding site.[9] We also explored the inclusion of various aliphatic sulfones and sulfonamides into the inhibitor design. As shown in Table 2, saturation of the terminal phenyl ring present in **8** afforded a compound (**22**) with encouraging NAMPT inhibition properties but unacceptably low stability in human liver microsomes. The poor in vitro stability of **22** could be improved by blocking metabolism on the cyclohexane ring (**23**) or by reducing compound lipophilicity through the incorporation of various polar functional groups in this region of the molecule (**24**–**31**). However, many of these modifications were also detrimental to anti-NAMPT potency in the biochemical and/or cell-based assessments. Compounds containing terminal sulfonamide moieties (**32**–**40**) were generally weaker NAMPT inhibitors than the related sulfones, but several exceptions to this trend were identified (**38**–**40**). With the exception of compound **22**, in vitro human liver microsomal stabilities for all compounds depicted in Table 2 were in the stable to moderate range. Measured aqueous solubilities were also generally favorable with many compounds displaying values >100 μM in the high-throughput assessment.[13]

In anticipation of conducting in vivo experiments with the described NAMPT inhibitors, we profiled selected examples in a variety of additional in vitro DMPK assessments. We focused these efforts on molecules which exhibited potent anti-NAMPT activity (A2780 $IC_{50} \leqslant 0.020$ μM), good in vitro stability toward human liver microsomes (HLM CL $\leqslant$ 10 mL/min/kg), and appropriate aqueous solubility (>50 μM in the high throughput assessment). As shown in Table 3, the majority of these compounds were not

Table 1
Initial structure–activity relationships

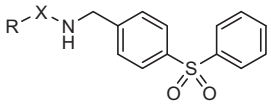

Compd	R	X	NAMPT IC50[a] (μM)	A2780 IC50[b] (μM)	Solubility[c] (μM)
5[d]	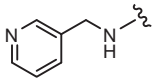	C=O	0.019	0.61	10
6	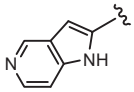	C=O	0.020	0.018	3
7	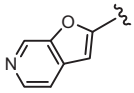	C=O	0.009	0.009	21
8	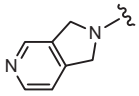	C=O	0.014	0.015	115
9	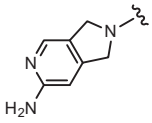	C=O	0.075	0.38	5.5
10	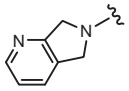	C=O	0.060	>2.0	144
11	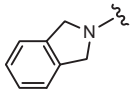	C=O	0.012	>2.0	1
12	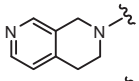	C=O	0.31	>2.0	115
13	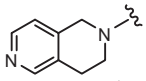	C=O	>2.0	>2.0	102
14	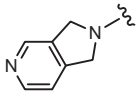	SO_2	>2.0	>2.0	3

All biochemical and cell-based assay results are reported as the arithmetic mean of at least two separate runs. Solubility determinations are $n = 1$. See supplementary data for experimental details associated with each assessment.

[a] NAMPT biochemical inhibition.

[b] Antiproliferation activity determined in cell culture experiments using A2780 cell line. This inhibition can be reversed by addition of 0.33 mM of NMN.

[c] Aqueous solubility.

[d] Contains piperidine derived sulfonamide in place of phenyl sulfone.

potent inhibitors of the cytochrome P450 (CYP) 3A4 isoform in both time-dependent and non-time-dependent assessments (two substrates examined). They also exhibited minimal inhibition of several other CYP isoforms (2D6, 1A2, 2C19) but were strong inhibitors of CYP2C9. Similar CYP2C9 inhibition properties were noted previously for related urea-containing NAMPT inhibitors.[6b] In contrast to their favorable stability toward human liver microsomes (Table 2), the optimized 2,3-dihydro-1*H*-pyrrolo[3,4-c]pyridine-derived ureas were relatively labile when tested in the presence of mouse liver microsomes (Table 4). However, all such compounds displayed improved stability properties when assessed using mouse hepatocytes (Table 4). The molecules also exhibited a range of in vitro permeability properties in MDCK cells, with those bearing polar substituents displaying the lowest (poorest) values (**19**, **28**, **29**; Table 4). Mouse plasma protein binding for the compounds was typically moderate (ca. 90% bound), although several molecules with significantly higher unbound fractions were also identified (**19**, **29**; Table 4). Collectively, the above assessments indicated that compound **18** possessed an ideal combination of potent NAMPT inhibition activity and attractive in vitro DMPK properties. The molecule also exhibited antiproliferative effects against a number of additional human tumor cell lines (Table 5), although in some instances such activity was slightly attenuated relative to potency against the A2780 line. Based on these favorable characteristics, compound **18** was therefore progressed to in vivo mouse PK and xenograft efficacy studies.

As shown in Figure 3 and Table 6, inhibitor **18** exhibited acceptable bioavailability and plasma exposure following oral administration to female NCR nude mice.[15] Single-dose IV administration of the compound determined that the molecule's in vivo mouse CL value resided somewhere in between those predicted from the in vitro mouse microsome and hepatocyte stability assessments (c.f., Tables 4 and 6). Importantly, BID administration of **18** at 40 mg/kg/dose afforded free mouse plasma levels which exceeded the compound's A2780 and PC-3 antiproliferation cell culture IC_{50} values for at least 12 h following the first dose (Fig. 3). Accordingly, compound **18** displayed significant efficacy in the NCI-PC3 human prostate cancer xenograft model with relatively

Table 2
Structure–activity relationships of 2,3-dihydro-1*H*-pyrrolo[3,4-c]pyridine-derived ureas

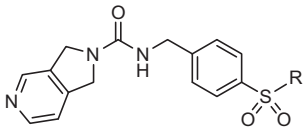

Compd	R	NAMPT IC50[a] (μM)	A2780 IC50[b] (μM)	HLM CLhep[c] (mL/min/kg)	Solubility[d] (μM)
8	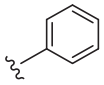	0.014	0.015	7.5	115
15	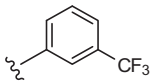	0.008	0.0027	14	10
16	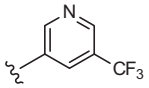	0.015	0.010	13	83
17	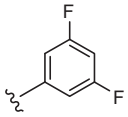	0.0071	0.0063	8	16
18	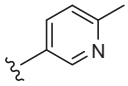	0.011	0.011	3.5	183
19	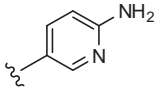	0.017	0.020	6	124
20	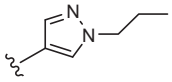	0.017	0.0073	11	105
21	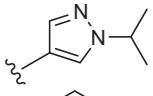	0.020	0.011	4	192
22	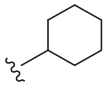	0.002	0.013	16	145
23	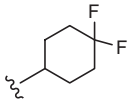	0.078	0.013	6	35
24	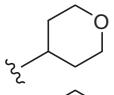	0.026	0.035	6	206
25[e]	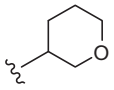	0.044	0.032	7	208
26	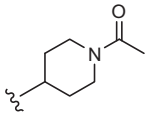	0.083	0.11	6	187
27	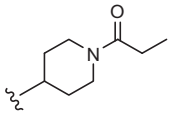	0.027	0.054	11	216
28	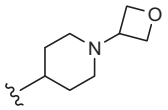	0.031	0.0074	10	121
29	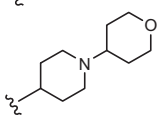	0.010	0.0070	5	214

Table 2 (*continued*)

Compd	R	NAMPT IC50[a] (μM)	A2780 IC50[b] (μM)	HLM CLhep[c] (mL/min/kg)	Solubility[d] (μM)
30	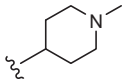	0.048	0.099	11	240
31	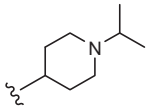	0.058	0.026	9	142
32	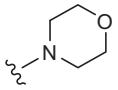	0.071	0.068	9	59
33	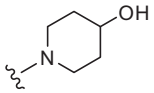	0.044	0.098	6	174
34[f]	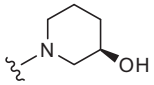	0.028	0.070	ND	216
35[f]	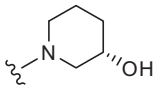	0.77	0.15	8	215
36	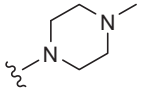	0.038	0.071	9	160
37	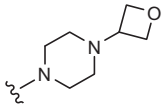	0.059	0.046	9	196
38	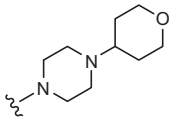	0.022	0.0095	13	194
39	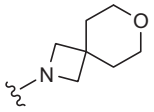	0.020	0.010	13	272
40	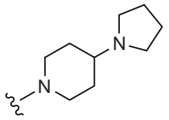	0.0074	0.0056	6	6.2

See supplementary data for experimental details associated with each assessment. All biochemical and cell-based assay results are reported as the arithmetic mean of at least two separate runs. Solubility and HLM determinations are $n = 1$.

[a] NAMPT biochemical inhibition.

[b] Antiproliferation activity determined in cell culture experiments using A2780 cell line. This inhibition can be reversed by addition of 0.33 mM of NMN.

[c] Human hepatic clearance predicted from human liver microsomes (stable, moderate, labile = <6, 6–15, >15 mL/min/kg, respectively).

[d] Aqueous solubility.

[e] Racemic mixture.

[f] Single enantiomer (unknown absolute configuration). ND = not determined.

Table 3
CYP inhibition properties of selected NAMPT inhibitors

Compd	Time-dependent CYP Inhib		CYP Inhib IC_{50}[c] (μM)					
	3A4 TDI (T) (% AUC shift)[a]	3A4 TDI (M) (% AUC shift)[b]	3A4 (T)	3A4 (M)	2D6	1A2	2C19	2C9
8	<15	<15	>10	>10	5–10	>10	3.7	0.054
18	23	<15	>10	>10	>10	>10	>10	0.077
19	<15	<15	>10	>10	>10	>10	6.2	0.065
21	<15	<15	>10	>10	>10	>10	6.2	0.073
28	<15	<15	>10	>10	>10	>10	>10	0.30
29	<15	<15	>10	>10	>10	>10	>10	0.27

See supplementary data for experimental details associated with each assessment. All assay results are reported as the arithmetic mean of at least two separate runs. ND = not determined.

[a] Time-dependent inhibition of 3A4 cytochrome P450 isoform (substrate = testosterone); >15% AUC shift considered possible TDI risk.

[b] Time-dependent inhibition of 3A4 cytochrome P450 isoform (substrate = midazolam); >15% AUC shift considered possible TDI risk.

[c] Cytochrome P450 inhibition activity (various isoforms; T = testosterone substrate, M = midazolam substrate).

Table 4
In vitro DMPK properties of selected NAMPT inhibitors

Compd	MLM CL_{hep}[a](mL/min/kg)	MH CL_{hep}[b](mL/min/kg)	MDCK $P_{app,A-B} \times 10^{-6}$ cm/s[c]	Mouse PPB (f_u)[d]
8	75	43	8.3	0.093
18	71	36	2.5	0.14
19	63	26	0.50	0.20
21	71	45	4.1	0.12
28	56	19	0.10	0.078
29	65	25	0.10	0.36

See supplementary data for experimental details associated with each assessment. All assay results are reported as the arithmetic mean of at least two separate runs.
[a] Mouse hepatic clearance predicted from mouse liver microsomes (stable, moderate, labile = <27, 27–63, >63 mL/min/kg, respectively).
[b] Mouse hepatic clearance predicted from mouse hepatocytes (stable, moderate, labile = <27, 27–63, >63 mL/min/kg, respectively).
[c] Apparent permeability coefficients ($P_{app,A-B}$) across MDCK cell monolayers.
[d] Mouse plasma protein binding; fraction unbound.

Table 5
Antiproliferation effects determined for compound **18** in various human tumor cell lines[a,b]

	HT1080	PC3	MiaPaCa2	HCT116
IC_{50} (nM)	25 ± 1	36 ± 19	70 ± 9	22 ± 4

[a] CyQuant endpoint; arithmetic mean of three separate runs ($n = 3$, standard deviations are also shown).
[b] All antiproliferation effects were reversed by addition of 330 μM NMN, strongly implicating NAMPT inhibition as the causative MOA. See Supplementary data for experimental details.

minor decreases in body weights (Fig. 4; see supplementary data for additional details).[15]

To enable further optimization of the described urea-containing series of NAMPT inhibitors, we obtained a crystal structure of compound **29** in complex with the NAMPT enzyme.[16] As shown in Figure 5, the compound made numerous favorable contacts with the protein. For example, the pyridine ring of the 2,3-dihydro-1*H*-pyrrolo[3,4-c]pyridine-derived urea moiety participated in an offset face-to-face pi-stack with the side chains of NAMPT residues Tyr18′ and Phe193. This binding location was previously observed to be occupied by the pyridine ring of the nicotinamide NAMPT substrate as well as by heterocycles associated with several other classes of NAMPT inhibitors.[6,9,17] The electron density of the NAMPT-**29** structure did not allow unambiguous orientation of the pyridine nitrogen atom. The depicted urea rotamer placed this atom within hydrogen bonding distance of a water molecule and

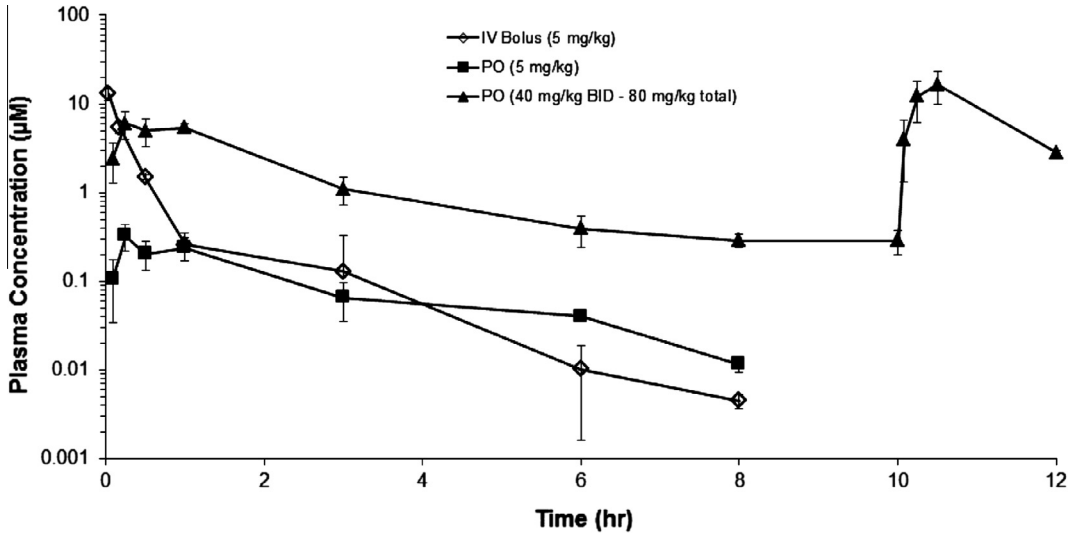

Figure 3. Mean (± standard deviation) plasma concentration-time profiles of compound **18** in female NCR nude mice following intravenous and oral administration.

Table 6
In vivo PK properties of compound **18** in nude mice.

Route	Dose[a] (mg/kg)	C_{max}[b] (μM)	T_{max}[c] (h)	Vss[d] (L/kg)	CL[e](mL/min/kg)	$T_{1/2}$[f] (h)	F[g] (%)
IV	5	—	—	2.04	57.7	1.12	—
PO	5	0.33	0.25	—	—	1.85	20.3

[a] Formulation = 35:10:15:40 PEG400:EtOH:PG:H_2O (solution).
[b] Maximum plasma concentration.
[c] Time at which maximum plasma concentration observed.
[d] Volume of distribution (steady-state).
[e] Clearance.
[f] Half-life.
[g] Bioavailibility. See supplementary data for experimental descriptions.

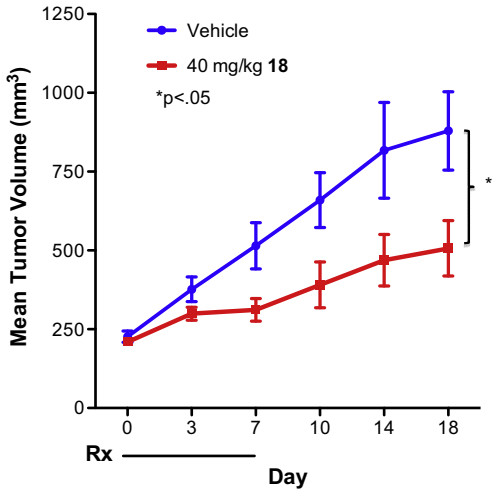

Figure 4. Efficacy of compound **18** (dosed 40 mg/kg BID) in the NCI-PC3 human prostate cancer xenograft model. Eight (8) mice were tested per group. Vehicle = 60% PEG400/10% EtOH/30% D5W. Data reflect mean tumor volumes (± standard error of mean).

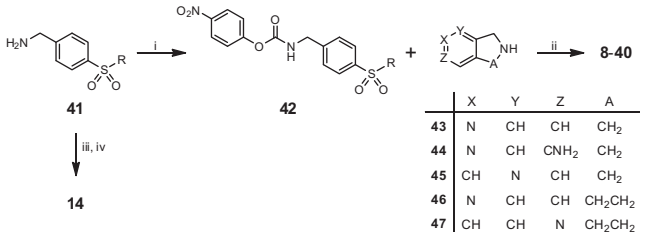

	X	Y	Z	A
43	N	CH	CH	CH_2
44	N	CH	CNH_2	CH_2
45	CH	N	CH	CH_2
46	N	CH	CH	CH_2CH_2
47	CH	CH	N	CH_2CH_2

Scheme 1. General synthesis of urea-containing compounds. Reagents and conditions: (i) $(4\text{-}NO_2)PhC(O)Cl$, toluene, 110 °C, 2 h; (ii) EtOH, reflux, 2 h, 45–82%; (iii) $OCNSO_2Cl$, 2-bromoethanol, CH_2Cl_2, 0 °C, 30 min; then **41**, *i*$PrNEt_2$ CH_2Cl_2, 0 °C, 40 min, 47%; (iv) **43**, CH_3CN, 70 °C, 14 h, 74%.

properly positioned it for reaction with the PRPP co-factor in the NAMPT active site.[14] The urea linkage of **29** extended into a polar portion of the substrate tunnel region and the urea NH formed a hydrogen bond with the side chain of Asp219. As shown in Figure 5, a water-mediated hydrogen bond was observed to bridge between the urea carbonyl oxygen of **29** and the side chain of Ser275. The benzylic portion of **29** formed favorable Van der Waals contacts with the more hydrophobic regions of the NAMPT substrate tunnel including the side chains of Val242 and Ile351. The central phenyl ring of the inhibitor phenyl ring also participated in a favorable edge-to-face pi interaction with the His191 side chain. The sulfone moiety of **29** made one hydrogen bond to a structural water molecule while the substituted piperidine fragment was highly solvent-exposed and made relatively few specific protein interactions. For example, Van der Waals contacts were noted only between the piperidine ring of **29** and Ile309 as well as between the ligand's tetrahydropyran ring and Pro307. A water molecule was also observed within hydrogen bonding distance of the piperidine nitrogen atom, although this entity was not present in the other ligand binding site contained in the NAMPT dimer.[16]

The inhibitors described in this work were prepared by the general method depicted in Scheme 1.[18] In this approach, various benzylic amines (**41**) were converted to their corresponding 4-nitro-phenyl carbamates (**42**) and these entities were subsequently condensed with bicyclic amines **43**–**47** to give the desired ureas.[19] With the exception of **44** (see below), the required bicyclic amines were commercially available and the preparations of **43**,[20] **45**,[21] and **46**[22] are also described in the literature. The sulfonyl urea **14** was prepared from amine **41** (R = Ph) and 2,3-dihydro-1*H*-pyrrolo[3,4-*c*]pyridine (**43**) by sequentially reacting the amine components with 2-oxo-1,3-oxazolidine-3-sulfonyl chloride generated in situ from 2-bromoethanol and chlorosulfonyl isocyanate.[23]

The synthesis of bicyclic amine **44** (required for the preparation of compound **9**) is depicted in Scheme 2.[24] 6-Chloronicotinic acid (**48**) was converted to the corresponding acyl chloride and this

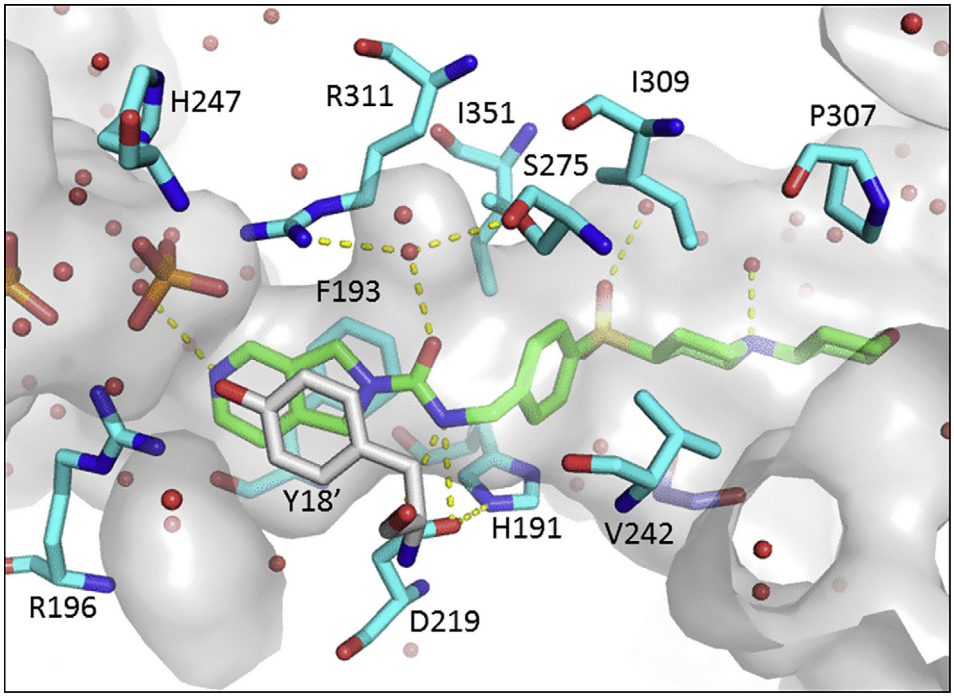

Figure 5. Co-crystal structure of inhibitor **29** (green) in complex with NAMPT. The ligand binds to a site formed by the interface of two NAMPT protein monomers (depicted as white and cyan, respectively). Water molecules are depicted as red spheres. Hydrogen bonds are indicated with dashed yellow lines, and the van der Waals surface of the protein is shown in grey. Two phosphates (orange), likely originating from the crystallization buffer, are also depicted. The resolution of the structure is 1.84 Å.

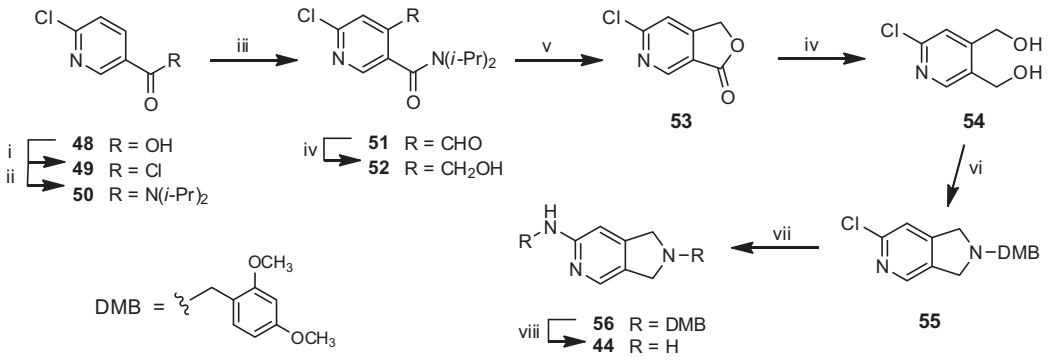

Scheme 2. Synthesis of amine **44**. Reagents and conditions: (i) $SOCl_2$, DMF, toluene, 85 °C, 5 h, 95%; (ii) $HN(i\text{-}Pr)_2$, DIEA, CH_2Cl_2, 10 °C, 2 h, 85%; (iii) LDA, HCOOEt, Et_2O, −75 °C, 1 h, 65%; (iv) $NaBH_4$, EtOH, 25 °C, 1 h, 78%; (v) HCl (6 M, aq), 120 °C, 2 h, 46%; (vi) $SOCl_2$, H_2N–DMB, CH_2Cl_2, 25 °C, overnight, 37%; (vii) $Pd_2(dba)_3$, dppf, H_2N–DMB, toluene, 90 °C, overnight, 58%; (viii) TFA, CH_2Cl_2, reflux, overnight, 52%.

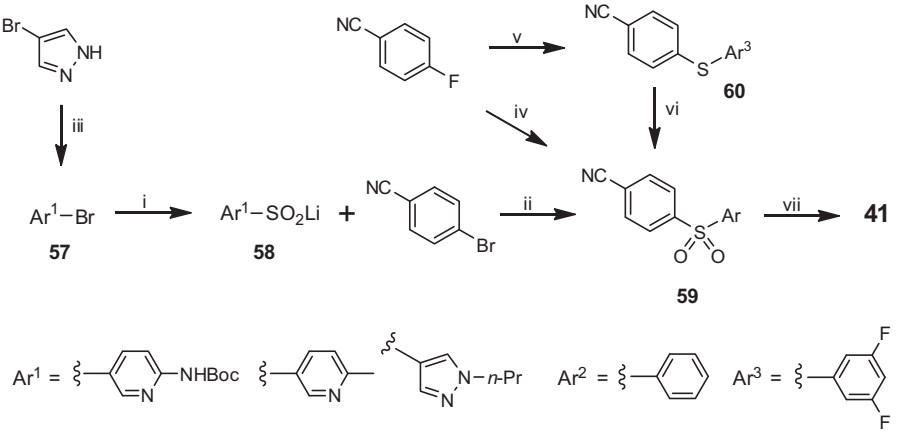

Scheme 3. Synthesis of amines **41** required to prepare compounds **8** and **17**–**20**. Reagents and conditions: (i) *n*-BuLi, SO_2, THF, −78 °C, 1 h, 93%; (ii) DMF, 120 °C, 16 h, 15%, (iii) *n*-PrBr, KOH, EtOH, 80 °C, 12 h; (iv) Ar^2SO_2Na, DMSO, 130 °C, 16 h, 94%; (v) Ar^3SH, K_2CO_3, DMF, 145 °C, 12 h, 89%; (vi) Oxone, CH_3CN/H_2O, 25 °C, 2 h, 81%; (vii) Raney Ni, 2 N NH_3 in CH_3OH, H_2, 25 °C, 1 h, 42–68%.

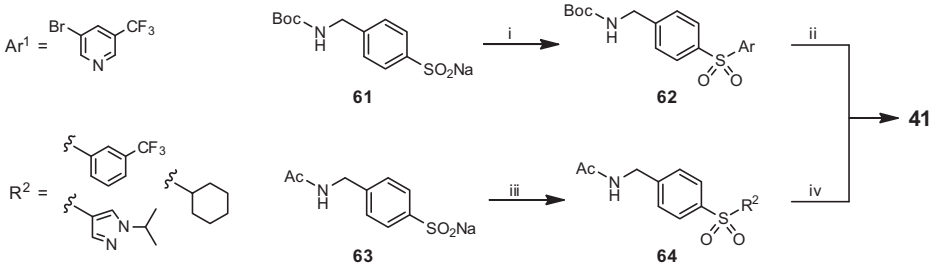

Scheme 4. Synthesis of amines **41** required to prepare compounds **15**, **16**, **21**, and **22**. Reagents and conditions: (i) Ar^1, DMSO, 120 °C, overnight, 8%; (ii) TFA, CH_2Cl_2, 25 °C, 40 min; (iii) R^2-$B(OH)_2$, $Cu(OAc)_2$, K_2CO_3 or Et_3N, DMSO, 60 °C, 16 h; (iv) 3.0 M HCl, *i*-PrOH, reflux, 16–48 h, 31–63%.

entity was subsequently condensed with *N*,*N*-diisopropylamine to afford amide **50**. Directed deprotonation of **50** with lithium diisopropylamide followed by trapping with ethyl formate provided aldehyde **51** which was then reduced to give the corresponding alcohol (**52**). Intramolecular cyclization of **52** was then accomplished under acidic conditions at elevated temperature and the resulting lactone (**53**) was subsequently reduced to afford diol **54**. After exposure of **54** to thionyl chloride, the resulting dichloride (not shown) was condensed with 2,4-dimethoxybenzylamine to provide amine **55**. A second 2,4-dimethoxybenzylamino substituent was then introduced using a palladium-catalyzed process to give intermediate **56**. Removal of both 2,4-dimethoxybenzyl moieties present in **56** under strongly acidic conditions afforded amine **44**.

The syntheses of the benzylic amines (**41**) required to prepare ureas **8**[22] and **17**–**20** are depicted in Scheme 3. Various aryl bromides (**57**) were converted to their corresponding lithium sulfinates (**58**) by *n*-butyllithium-mediated metal–halogen exchange followed by trapping with sulfur dioxide gas.[25] The sulfinates were subsequently coupled with 4-bromobenzonitrile at elevated temperature to give various cyano-containing sulfones (**59**).[26] Reduction of the cyano groups present in these entities with hydrogen/Raney nickel[27] afforded the desired amines (**41**). The aryl bromide **57** required for the synthesis of inhibitor **20** was prepared by alkylation of 4-bromo-1*H*-pyrazole.[28] Two alternate syntheses of sulfones **59** are also depicted in Scheme 3. In the first method, 4-fluorobenzonitrile was condensed with commercially available

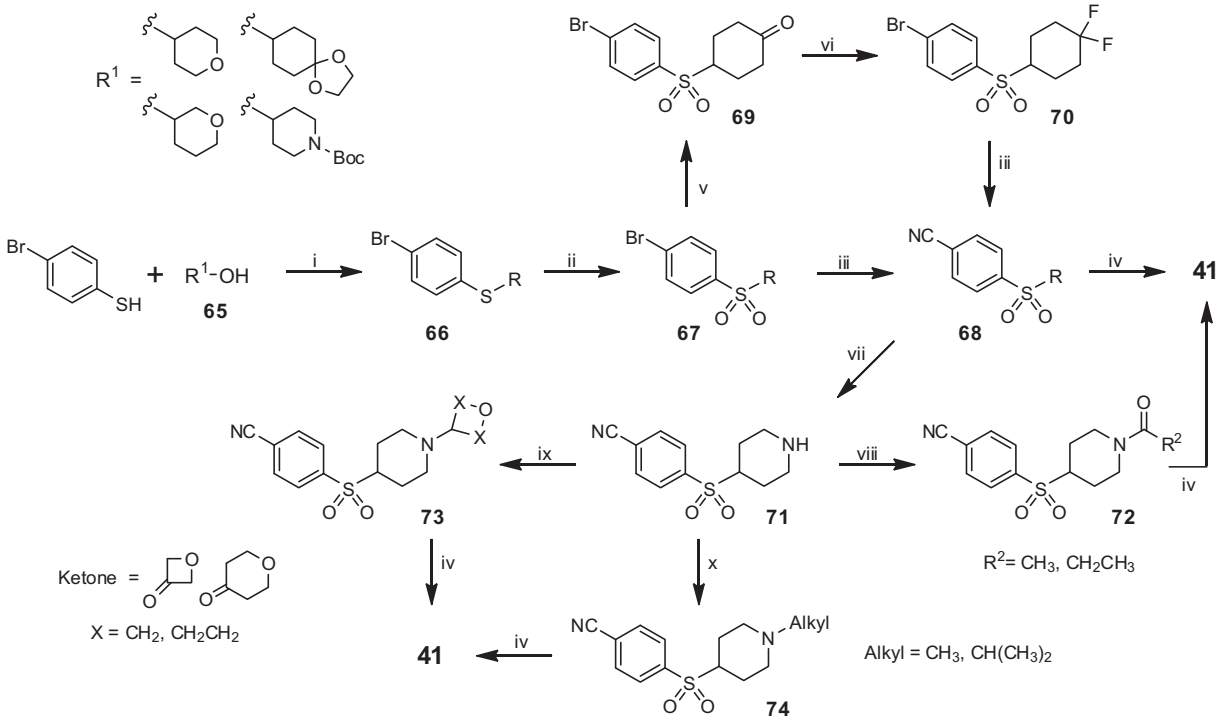

Scheme 5. Synthesis of amines **41** required to prepare compounds **23**–**31**. Reagents and conditions: (i) DIAD, PPh_3, THF, 25 °C, 12 h, 41%; (ii) *m*-CPBA, $CHCl_3$, 25 °C, 5 h, 81%; (iii) $Pd_2(dba)_3$, dppf, $ZnCN_2$, DMF, 120 °C, 12 h, 77%; (iv) Raney Ni, 2N NH_3 in CH_3OH, H_2, 25 °C, 1 h, 59–69%; (v) HCl (2 M, aq), H_2O, 60 °C, 3 h, 79%; (vi) DAST, CH_2Cl_2, 25 °C, 5 h, 36%; (vii) TFA, CH_2Cl_2, 25 °C, 5 h, 83%; (viii) RCOCl, (*i*-Pr)$_2$NEt, CH_2Cl_2, 25 °C, 1 h, 92–94%; (ix) Ketone, $Ti(OEt)_4$, $NaBH_3CN$, AcOH, EtOH, 60 °C, 12 h, 62–78%; (x) CH_2O or acetone, $NaBH_3CN$, AcOH, EtOH, 60 °C, 12 h, 42–67%.

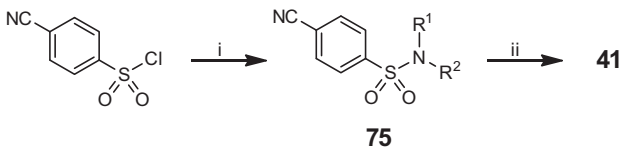

Scheme 6. Synthesis of amines **41** required to prepare compounds **32**–**40**. Reagents and conditions: (i) Et_3N, HNR^1R^2, CH_2Cl_2, 25 °C, 2 h, 67–85%; (ii) Raney Ni, 2 N NH_3 in CH_3OH, H_2, 25 °C, 1 h, 82–98%.

sodium benzenesulfinate to afford the desired sulfone (**59**, Ar = Ph).[29] In the second method, 4-fluorobenzonitrile was reacted with 3,5-difluorobenzenethiol to give the sulfide **60**. This entity was subsequently oxidized to the corresponding sulfone (**59**, Ar = 3,5-di-F–Ph) by treatment with Oxone.

The syntheses of the benzylic amines (**41**) required to prepare ureas **15**, **16**, **21**, and **22** are depicted in Scheme 4. Sulfinate intermediate **61**[9] was condensed with 3-bromo-5-(trifluoromethyl)pyridine to give sulfone **62** (Ar = 3-pyridyl-5-trifluoromethyl).[26] Deprotection of the N-Boc moiety present in **62** under acidic conditions then afforded the desired amine **41**. Similarly, sulfinate intermediate **63**[29] was coupled with a variety of boronic acids to give the corresponding sulfones **64**.[26] Deprotection of the *N*-acetyl moiety present in **64** under acidic conditions subsequently afforded the desired amines **41**.

The syntheses of the benzylic amines (**41**) required to prepare ureas **23**–**31** are depicted in Scheme 5. 4-Bromobenzenethiol was coupled under Mitsunobu conditions with a variety of secondary alcohols to give sulfides **66**.[30] These entities were oxidized to the corresponding sulfones, and the bromides present in these oxidized molecules were replaced with nitrile groups using palladium-catalyzed transformations (providing intermediates **68**).[31] As described in Scheme 3 above, reduction of the cyano groups present in the tetrahydropyran-containing intermediates **68** with hydrogen/Raney nickel[27] afforded the desired amines (**41**). The amine **41** required to synthesize difluoro-containing inhibitor **23** was prepared by acidic deprotection of the dioxolane-containing intermediate **67** to give cyclohexanone **69**. Reaction of **69** with (diethylamino)sulfur trifluoride (DAST) afforded intermediate **70** which was transformed to the corresponding nitrile **68** (and subsequently amine **41**) by the methods described above. The amines **41** required to synthesize inhibitors **26** and **27** were prepared by removal of the Boc protecting group present in the piperidine-containing intermediate **68** under acidic conditions followed by derivitization of the free amine (**71**) with various acid chlorides. The resulting acylated intermediates (**72**) were reduced as described above to give the desired amines **41**. Similarly, the alkylated piperidines (**41**) required for the syntheses of inhibitors **28**–**31** were prepared by alkylation or reductive amination of intermediate **71** followed by nitrile reduction as previously described.

The syntheses of the sulfonamide-containing benzylic amines (**41**) required to prepare ureas **32**–**40** are depicted in Scheme 6. Commercially available 4-cyanobenzene-1-sulfonyl chloride was condensed with a variety of commercially available amines to give the corresponding sulfonamides (**75**). Reduction of the nitrile moieties present in **75** using the hydrogen/Raney nickel procedure described in several other synthesis Schemes then afforded the desired amines **41**.

Acknowledgements

We thank Drs. Krista Bowman and Jiansheng Wu and their respective Genentech research groups for performing many protein expression and purification activities, the DMPK group at Genentech, especially Jonathan Cheong, Erlie Marie Delarosa, Suzanne Tay, Jasleen Sodhi, and Ning Liu for their contributions

to the generation of the in vitro DMPK data, the Genentech in vivo cell culture core and in vivo Pharmacology dosing technicians for their support of the efficacy studies, Rashida Garcia-Dancey and Shohini Ganguly for helping to generate the cellular data, and Agilent Technologies (Woburn, MA) for generating the Rapidfire LCMS data. We also thank Dr. Peter Jackson for many helpful discussions regarding NAMPT.

Supplementary data

Supplementary data associated with this article can be found, in the online version, at http://dx.doi.org/10.1016/j.bmcl.2013.06.090.

References and notes

1. (a) He, J.; Tu, C.; Li, M.; Wang, S.; Guan, X.; Lin, J.; Li, Z. *Curr. Pharm. Des.* **2012**, *18*, 6123; (b) Burgos, E. S. *Curr. Med. Chem.* **1947**, *2011*, 18; (c) Bi, T.-Q.; Che, X.-M. *Cancer Biol. Ther.* **2010**, *10*, 119; (d) Garten, A.; Petzold, S.; Körner, A.; Imai, S.-I.; Kiess, W. *Trends Endocrinol. Metab.* **2008**, *20*, 130.
2. (a) Houtkooper, R. H.; Cantó, C.; Wanders, R. J.; Auwerx, J. *Endocr. Rev.* **2010**, *31*, 194; (b) Sauve, A. A. *J. Pharmacol. Exp. Ther.* **2008**, *324*, 883.
3. In contrast, the de novo NAD synthesis pathway requires eight enzyme-catalyzed steps to produce the co-factor from tryptophan. See Ref. 2 for additional details.
4. (a) Schulze, A.; Harris, A. L. *Nature* **2012**, *491*, 364; (b) Chiarugi, A.; Dölle, C.; Felici, R.; Ziegler, M. *Nat. Rev. Cancer* **2012**, *12*, 741; (c) Zhang, L. Q.; Heruth, D. P.; Ye, S. Q. *J. Bioanal. Biomed.* **2011**, *3*, 13; (d) Khan, J. A.; Forouhar, F.; Tao, X.; Tong, L. *Expert Opin. Ther. Targets* **2007**, *11*, 695.
5. Two NAMPT inhibitors have been progressed to human clinical trials: (a) Watson, M.; Roulston, A.; Bélec, L.; Billot, X.; Marcellus, R.; Bédard, D.; Bernier, C.; Branchaud, S.; Chan, H.; Dairi, K.; Gilbert, K.; Goulet, D.; Gratton, M.-O.; Isakau, H.; Jang, A.; Khadir, A.; Koch, E.; Lavoie, M.; Lawless, M.; Nguyen, M.; Paquette, D.; Turcotte, E.; Berger, A.; Mitchell, M.; Shore, G. C.; Beauparlant, P. *Mol. Cell. Biol.* **2009**, *29*, 5872; (b) Ravaud, A.; Cerny, T.; Terret, C.; Wanders, J.; Bui, B. N.; Hess, D.; Droz, J.-P.; Fumoleau, P.; Twelves, C. *Eur. J. Cancer* **2005**, *41*, 702; (c) Hovstadius, P.; Larsson, R.; Jonsson, E.; Skov, T.; Kissmeyer, A.-M.; Krasilnikoff, K.; Bergh, J.; Karlsson, M. O.; Lönnebo, A.; Ahlgren, J. *Clin. Cancer Res.* **2002**, *8*, 2843; (d) Olesen, U. H.; Thougaard, A. V.; Jensen, P. B.; Sehested, M. *Mol. Cancer Ther.* **2010**, *9*, 1609; (e) Holen, K.; Saltz, L. B.; Hollywood, E.; Burk, K.; Hanauske, A.-R. *Invest. New Drugs* **2008**, *26*, 45.
6. (a) Zheng, X.; Bauer, P.; Baumeister, T.; Buckmelter, A. J.; Caligiuri, M.; Clodfelter, K. H.; Han, B.; Ho, Y.-C.; Kley, N.; Lin, J.; Reynolds, D. J.; Sharma, G.; Smith, C. C.; Wang, Z.; Dragovich, P. S.; Oh, A.; Wang, W.; Zak, M.; Gunzner-Toste, J.; Zhao, G.; Yuen, P. W.; Bair, K. W *J. Med. Chem.* **2013**, *56*, 4921; (b) Gunzner-Toste, J.; Zhao, G.; Bauer, P.; Baumeister, T.; Buckmelter, A. J.; Caligiuri, M.; Clodfelter, K. H.; Fu, B.; Han, B.; Ho, Y.-C.; Kley, N.; Liang, X.; Liederer, B.; Lin, J.; Mukadam, S.; O'Brien, T.; Reynolds, D. J.; Sharma, G.; Skelton, N.; Smith, C. C.; Wang, W.; Wang, Z.; Xiao, Y.; Yuen, P. W.; Zak, M.; Zhang, L.; Zheng, X.; Bair, K. W.; Dragovich, P. S *Bioorg. Med. Chem. Lett.* **2013**, *23*, 3531.
7. (a) For other examples of urea-containing NAMPT inhibitors, see: Kumar, D. V.; Slattum, P. M.; Yager, K. M.; Shenderovich, M. D.; Tangallapally, R.; Kim, S. -H. WO 2012/177782.; (b) Willardsen, A. J.; Lockman, J. W.; Murphy, B. R.; Judd, W. R.; Kim, I. C.; Kim, S. -H.; Zigar, D. F.; Yager, K. M.; Fleischer, T. C.; Terry-Lorenzo, R. T.; Boniface, J. J.; Parker, D. P.; McAlexander, I. A.; Bursavich, M. G.; Dastrup, D. M. WO 2011/109441.; (c) Arigon, J.; Bernhart, C.; Bouaboula, M.; Dimalta, A.; Nardi, F.; Jegham, S.; Roux, R. WO 2012/038904.; (d) Bernhart, C.; Bouaboula, M.; Casellas, P.; Jegham, S.; Arigon, J.; Combet, R.; Hilairet, S.; Fraisse, P. US 2010/0222319.
8. For additional examples of NAMPT inhibitors, see: (a) You, H.; Youn, H.-S.; Im, I.; Bae, M.-H.; Lee, S.-K.; Ko, H.; Eom, S. H.; Kim, Y.-C. *Eur. J. Med. Chem.* **2011**, *46*, 1153; (b) Lockman, J. W.; Murphy, B. R.; Zigar, D. F.; Judd, W. R.; Slattum, P. M.; Gao, Z.-H.; Ostanin, K.; Green, J.; McKinnon, R.; Terry-Lorenzo, R. T.; Fleischer, T. C.; Boniface, J. J.; Shenderovich, M.; Willardsen, J. A. *J. Med. Chem.* **2010**, *53*, 8734; (c) Colombano, G.; Travelli, C.; Galli, U.; Caldarelli, A.; Chini, M. G.; Canonico, P. L.; Sorba, G.; Bifulco, G.; Tron, G. C.; Genazzani, A. A. *J. Med. Chem.* **2010**, *53*, 616.
9. Zheng, X.; Bauer, P.; Baumeister, T.; Buckmelter, A. J.; Caligiuri, M.; Clodfelter, K. H.; Han, B.; Ho, Y. -C.; Kley, N.; Lin, J.; Reynolds, D. J.; Sharma, G.; Smith, C. C.; Wang, Z.; Dragovich, P. S.; Gunzner-Toste, J.; Liederer, B. M.; Ly. J.; O'Brien, T.; Oh, A.; Wang, L.; Wang, W.; Xiao, Y.; Zak, M.; Zhao, G.; Yuen, P. -w.; Bair, K. W. *J. Med. Chem.*, DOI: 10.1021/jm4008664.
10. Hill, A. P.; Young, R. J. *Drug Discovery Today* **2010**, *15*, 648.
11. (a) For examples of related NAMPT inhibitors containing ureas derived from cyclic, aliphatic amines, see Curtin, M. L.; Sorensen, B. K.; Heyman, H. R.; Clark, R. F.; Woller, K. R.; Shah, O. J.; Michaelides, M.; Tse, C.; Vasudevan, A.; Mack, H.; Hansen, T. M.; Sweis. R.; Pliushchev, M. A. US 2012/0122842.; (b) Curtin, M. L.; Sorensen, B. K.; Heyman, H. R.; Clark, R. F.; Michaelides, M.; Tse, C. US 2012/0122924.
12. The antiproliferative effects exhibited in cell culture by **8** were completely eliminated ("reversed") when the compound was tested in the presence of 0.33 mM NMN (the product of the NAMPT-catalyzed condensation of nicotinamide and PRPP; c.f.,. Fig. 1). This result strongly suggests that the observed cell-based effects result from NAMPT inhibition. Related NMN experiments were conducted in cell-based assessments with all inhibitors reported in this work and all displayed similar reversals of their antiproliferative effects.
13. Aqueous solubilities were determined using a 24-hour high-throughput assay employing DMSO compound solutions (see Supplementary data for additional details). Accordingly, the reported aqueous solubilities are best utilized as surrogates for more accurate (thermodynamic) solubility measurements determined using crystalline materials. Our experience with both assessments suggests that the high-throughput solubility values are unlikely to improve with subsequent compound scale-up and that deprioritization of compounds which perform poorly in the high-throughput assay is an effective strategy to identify molecules with acceptable solubility properties.
14. We currently believe that many cell-potent NAMPT inhibitors form PRPP-derived phosphoribosylated adducts in the protein's active site which block the function of the enzyme. This belief is consistent with the repeated observation of these adducts by mass spectrometry in biochemical experiments (see Refs. 5a,6,9). It is also consistent with the inability to detect similar adduct formation in related experiments with compound **10** (see Supplementary data) and another cell-inactive compound that was nevertheless a potent biochemical NAMPT inhibitor (Ref. 6). Once formed, the PRPP-adducts may accumulate intracellularly and thereby enhance cell culture antiproliferation effects (see Ref. 5a for additional information and discussion). However, there are many other factors that also likely influence NAMPT inhibitor cell potency including: biochemical potency, the ability of a given inhibitor and/or its corresponding PRPP-derived ribose adduct to effectively compete with the NAM substrate, cell membrane permeability, and/or protein binding. In addition, performing the PRPP-adduct assessments was a relatively resource-intensive task and such determinations were therefore made for only a small number of compounds.
15. To better accommodate work schedules, the second dose of compound **18** was given 10 h after the first dose on each day during the xenograft experiment. Mouse PK parameters were determined using a similar dosing schedule.
16. NAMPT is believed to function as a symmetrical homodimer with two active sites formed at opposite ends of the dimer interface. Accordingly, the protein crystallized with such a dimer present in the asymmetric unit. The two monomer chains in the dimer were very similar, having an RMSD of only 0.12 Å for 420 C-alpha atoms, and both active sites contained a molecule of compound **29** in a similar orientation. In the crystallography discussion, the NAMPT residues are designated with prime and non-prime notation (e.g., Tyr18′, Phe193) to distinguish the monomer chain in which a given residue resides. In addition, the electron density clearly defined multiple inorganic phosphates that likely originated from the crystallization buffer. See deposited PDB file for additional structural details: code = 4KFP.
17. (a) Burgos, E. S.; Ho, M.-C.; Almo, S. C.; Schramm, V. L. *Proc. Natl. Acad. Sci. USA* **2009**, *106*, 13748; Wang, T.; Zhang, X.; Bheda, P.; Revollo, J. R.; Imai, S.-I.; Wolberger, C. *Nat. Struct. Mol. Biol.* **2006**, *13*, 661; (c) Khan, J. A.; Tao, X.; Tong, L. *Nat. Struct. Mol. Biol.* **2006**, *13*, 582.
18. The chemical purities of all final compounds described in this work were >95% at the time of their biological assessments as determined by LCMS analysis with UV detection at 220 nm. We also noted, however, that some molecules containing the 2,3-dihydro-1*H*-pyrrolo[3,4-c]pyridine-derived urea moiety experienced oxidation upon prolonged storage (>1 month; particularly when stored in solvated form; detected via LCMS analysis of stored materials). No attempts were made to study or suppress this process and the oxidized compounds were neither isolated nor biologically characterized. LCMS fragmentation patterns suggested the oxidation products depicted below, but no additional analyses were conducted to confirm these assignments.

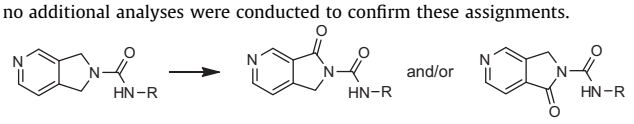

19. (a) Jiang, Y.; Chai, X.; Zou, Y.; Wu, Q.; Zhang, D.; Sun, Q.; Cao, Y.; Jiang, Y.; Zhang, J. *Bioorg. Med. Chem. Lett.* **2011**, *21*, 4471; (b) Mallakpour, S.; Rafiee, Z. *Synth. Commun.* **1927**, *2007*, 37.
20. Paget, S. D.; Foleno, B. D.; Boggs, C. M.; Goldschmidt, R. M.; Hlasta, D. J.; Weidner-Wells, M. A.; Werblood, H. M.; Wira, E.; Bush, K.; Macielag, M. J. *Bioorg. Med. Chem. Lett.* **2003**, *13*, 4173.
21. Paget, S. D.; Boggs, C. M.; Foleno, B. D.; Goldschmidt, R. M.; Hlasta, D. J.; Weidner-Wells, M. A.; Werblood, H. M.; Bush, K.; Macielag, M. J. *Bioorg. Med. Chem. Lett.* **2006**, *16*, 4537.
22. Dukat, M.; Fiedler, W.; Dumas, D.; Damaj, I.; Martin, B. R.; Rosecrans, J. A.; James, J. R.; Glennon, R. A. *Eur. J. Med. Chem.* **1996**, *31*, 875.
23. Borghese, A.; Antoine, L.; Van Hoeck, J. P.; Mockel, A.; Merschaert, A. *Org. Process Res. Dev.* **2006**, *10*, 770.
24. Blauen, S. J.; Narquizian, R.; Norcross, R. D., Olsberg; Pinard, E. US 2006/0178381.
25. Reggelin, M.; Gerlach, M.; Vogt, M. *Eur. J. Org. Chem.* **1999**, 1011.
26. Ulman, A.; Urankar, E. *J. Org. Chem.* **1989**, *54*, 4691.
27. (a) Depreux, P.; Lesieur, D.; Mansour, H. A.; Morgan, P.; Howell, H. E.; Renard, P.; Caignard, D.-H.; Pfeiffer, B.; Delagrange, P.; Guardiola, B.; Yous, S.; Demarque, A.; Adam, G.; Andrieux, J. *J. Med. Chem.* **1994**, *37*, 3231; (b) Amon, M.; Ligneau, X.; Schwartz, J.-C.; Stark, H. *Bioorg. Med. Chem. Lett.* **1938**, *2006*, 16.

28. Ivachtchenko, A. V.; Kravchenko, D. V.; Zheludeva, V. I.; Pershin, D. G. *J. Heterocycl. Chem.* **2004**, *41*, 931.
29. Bair, K. W.; Baumeister, T.; Buckmelter, A. J.; Clodfelter, K. H.; Dragovich, P. S.; Gosselin, F.; Han, B.; Lin, J.; Reynolds, D. J.; Roth, B.; Smith, C. C.; Wang, Z.; Yuen, P. -w.; Zheng, X. WO 2012/031197.
30. (a) Chapman, W. H.; Breslow, R. *J. Am. Chem. Soc.* **1995**, *117*, 5462; (b) Loibner, H.; Zbiral, E. *Helv. Chim. Acta* **1976**, *59*, 2100.
31. (a) Alterman, M.; Anders, H. *J. Org. Chem.* **2000**, *65*, 7984; (b) Chidambaram, R. *Tetrahedron Lett.* **2004**, *45*, 1441.
32. For a recent and broad review of NAMPT and many different classes of inhibitors, see: Galli, U.; Travelli, C.; Massarotti, A.; Fakhfouri, G.; Rahimian, R.; Tron, G. C.; Genazzani, A. A. *J. Med. Chem.* **2013**. http://dx.doi.org/10.1021/jm4001049.